Alfvén Eigenmodes and Alpha-Particle Losses in JET

W Kerner, L C Appel[1], M Cox[1], T C Hender[1], G T A Huysmans, M R O'Brien[1], S D Pinches[2], S E Sharapov[3], F S Zaitsev[4].

JET Joint Undertaking, Abingdon, Oxfordshire, OX14 3EA, UK.
[1] UKAEA/EURATOM Fusion Association, Culham, Abingdon, Oxfordshire, UK.
[2] University of Nottingham, Nottingham, UK.
[3] RRC Kurchatov Institute, Moscow, Russia.
[4] Moscow State University, Moscow, Russia.

"This document is intended for publication in the open literature. It is made available on the understanding that it may not be further circulated and extracts may not be published prior to publication of the original, without the consent of the Publications Officer, JET Joint Undertaking, Abingdon, Oxon, OX14 3EA, UK".

"Enquiries about Copyright and reproduction should be addressed to the Publications Officer, JET Joint Undertaking, Abingdon, Oxon, OX14 3EA".

ALFVEN EIGENMODES AND ALPHA-PARTICLE LOSSES IN JET

W. Kerner, L.C.Appel[1], M.Cox[1], T.C.Hender[1], G.T.A.Huysmans, M.R.O'Brien[1], S.D.Pinches[2], S.E.Sharapov[3], and F.S.Zaitsev[4]

JET Joint Undertaking, Abingdon, Oxon, OX14 3EA, UK.
[1]UKAEA/EURATOM Fusion Association, Culham, Abingdon, Oxon, UK.
[2]University of Nottingham, Nottingham, UK.
[3]RRC Kurchatov Institute, Moscow, Russia.
[4]Moscow State University, Moscow, Russia.

ABSTRACT

Fast α-particle losses in JET D-T discharges are studied in the context of neoclassical transport and anomalous losses of super-Alfvénic α-particles in the presence of unstable TAE's. It is found that in the Fokker-Planck treatment large orbit width effects need to be taken into account which leads to broader n_α profiles. In high performance JET discharges with $n_D \approx n_T$, typically, $n = 3$ TAE can be driven unstable. Such instabilities cause prompt α-losses scaling linearly with the TAE amplitude. Above the stochasticity threshold, which is fairly high in this case, anomalous α-particle diffusion sets in.

1. INTRODUCTION

The physics of α-particles in tokamaks is of particular interest and importance now that research into controlled fusion has reached thermonuclear parameters and D-T fuel has been used in JET and TFTR. One key issue for burning plasmas is transport. The magnitude of slow α-particle transport will determine the "Helium ash" content and therefore the dilution of the plasma. The level of fast α-particle transport, which is considered in this paper, will determine both the radial dependence of the source of Helium ash and the plasma heating profile. Studies of α-particle transport and losses feature in the TFTR D-T campaign [1] and are likely to feature in further D-T experiments in JET. In this paper we consider, for typical JET conditions, firstly fast α-particle neo-classical transport allowing for large drift orbit effects. Secondly, anomalous losses of super-Alfvénic α-particles in the presence of unstable TAE-modes are studied. The relevance of TAE-excitation in actual JET discharges can be verified experimentally by the Alfvén Eigenmode Active Diagnostic experiments in JET [2]. However, the problem whether unstable TAE's can cause significant anomalous losses of α-particles is of principal interest in itself. For this purpose we suppose some TAE's to be driven unstable and analyse the α-particle behaviour in the presence of finite-amplitude TAE's.

2. NEO-CLASSICAL ALPHA-PARTICLE TRANSPORT

The α-particle distribution f_α is calculated as a function of position, speed and pitch-angle using the FPP code [3]. The code solves the 3D trajectory-averaged Fokker-Planck equation [4] with terms for the α-particle source and the full collision operator including the neo-classical transport terms. The code has been tested by comparison with standard expressions for neo-classical ion fluxes, bootstrap current and toroidal conductivity, but is not restricted to large aspect ratios nor to distributions close to Maxwellian, unlike most neo-classical treatments. The collision operator can be integrated either over the full α-particle trajectories or over flux surfaces allowing an assessment of the importance of finite drift effects. Collisions are with background electron, deuterium and tritium Maxwellians. The α-particle source is isotropic in pitch-angle and monoenergetic (at 3.5MeV) with magnitude and profile determined by the background deuterium and tritium density and temperature profiles. Here we restrict the source to thermal-thermal fusion and neglect orbit losses. Also, the results here are steady-state, though a time-dependent simulation is used for the TFTR comparison and may be necessary for similar JET

comparisons. Parameters typical of JET were used for the simulations : R=3m; a=1.07m; κ=1.5; I_p=1, 3 and 5 MA; B_ϕ=3T; $n_e(r)=(0.9(1-r^2/a^2)^{1/2}+0.1)\ 5x10^{19}m^{-3}$; $n_D=n_T=0.4n_e$; $T_e(r)=(0.95(1-r^2/a^2)+0.05)$ x 10 keV; $T_D=T_T=2T_e$; $j(r)\sim(1-(r/a)^2)^2$ (which gives $q_o\sim1$ for I_p=3MA). Figure 1 shows the predicted profiles of α-particle density and plasma heating by the α-particles (which is largely electron heating) for I_p=1 and 3 MA.

On each graph the results of calculations with both flux surface- and trajectory-averaging are shown. As expected, the α-particle density rises with increasing I_p as the neo-classical transport drops. Also, the differences between surface- and trajectory-averaging reduce as I_p rises since the orbit widths drop. The trajectory-averaging gives a broader $n_\alpha(r)$ demonstrating the importance of including all large orbit width effects in the calculation. In the cases considered the transport time was long compared with the collision time and the α-particles had almost thermalised (energies $\sim10^2$ keV) by the time they left the plasma edge. Consequently the heating profile if orbit excursions are neglected is close to that deduced from the α-particle source (Figures 1(b) and 1(d)), though the orbit excursions significantly broaden the profile. These trends were confirmed by calculations for I_p=5MA (not illustrated).

Figure 2 shows, for the trajectory-averaged I_p=3MA case, velocity space contours of f_α at the inside and outside of the flux surface with r≈a/2. There is significant anisotropy in pitch-angle, unlike in standard slowing down approximations for f_α, showing that such approximations are inadequate for comparisons with α-particle measurements and that a fuller treatment as described here is required.

3. ALFVEN EIGENMODE SPECTRA AND PARTICLE LOSSES

In order to analyse the super-Alfvénic α-particle losses due to TAE's, the most unstable TAE's need to be identified. For typical JET parameters we calculate TAE-spectra, mode structure and continuum damping effect using the toroidal linear spectral code CASTOR [5]. For the analysis of driving and various damping mechanisms (ion Landau [6], trapped electron collisional [7,8] and radiative [9] dampings) a hybrid kinetic - MHD model is employed. The local TAE-stability analysis reveals that for low-m TAE-modes in JET ion Landau damping plays a dominant role; high-m TAE's are strongly suppressed by radiative and trapped electron collisional damping effects, and therefore TAE's of intermediate mode numbers, $m \sim 3 \div 6$, are the most dangerous. In particular, the TAE stability of a high performance deuterium JET discharge (#26087) was analysed, assuming $n_D = n_T$. It is found for this case that a modest decrease in density (and increase in temperature) destabilises the Alfven modes, and thus would permit their effects to be studied. The most likely candidates for TAE instability are found to be the n=3 modes. These n=3 eigenfunctions are used as input to a Hamiltonian guiding centre code with which collisionless losses due to TAE modes have been studied by Monte-Carlo simulations of 50,000 α-particles. The α-particles have a slowing down distribution with energies in the range 3.5MeV to 1.5MeV, a radial distribution varying as $(1-\Psi)^3$ and a random distribution in pitch, poloidal and toroidal angle. For these studies three n=3 TAE modes with normalised frequencies ω/ω_A=0.41, 0.51 and 0.58 have been used. Since these eigenmodes have been obtained from a linear simulation their amplitudes are arbitrary; here they are normalised so each eigenfunction has the same maximum radial field amplitude. As in Ref. [10] these Monte-Carlo simulations show two distinct classes of lost particles due to the n=3 TAE modes. Firstly there is a prompt loss of α-particles born near a loss boundary; co- and counter-passing particle prompt losses peak at ~3μs and trapped losses at ~6μs. These losses scale linearly with the applied TAE perturbation. Secondly above a stochastic threshold there is a steady long term loss of α-particles by stochastic diffusion into a loss boundary.

It can be seen from Fig 3 (d) that the majority of particles are lost just below the outboard mid-plane for the particular ∇B-drift direction used; this is due mainly to co-directed trapped particle orbits (see Fig 3(c)) intercepting the 'wall' (at $\theta \lesssim 0$).

We now examine the stochastic losses and diffusion in more detail. For passing particles the stochastic diffusion occurs in the presence of the TAE perturbations because the particle orbits and flux surfaces are relatively displaced causing side-band resonances. Stochasticity occurs when the particle excursions due to the primary and side-band [11] resonances overlap. With multiple TAE perturbations (of different frequency) stochasticity must be determined by the particle diffusion (or loss) which the TAE perturbations cause. As in Ref. [10] diffusion is measured by evaluating for an initially mono-energetic and mono-P_ϕ particle distribution, the spread of $\langle \Delta P_\phi^2 \rangle = \langle P_\phi^2 \rangle - \langle P_\phi \rangle^2$ in time (where $\langle\rangle$ denotes an ensemble average). Figure 4 (a) shows for the same n=3 TAE perturbations as used for Fig 3 the variation of $\langle \Delta P_\phi^2 \rangle$ with time for $\delta B_r/B=3x10^{-3}$ and $5x10^{-4}$; for these cases 500 particles are launched with an initial E=2.5MeV, $P_\phi=3.6x10^{-19}kgm^2s^{-1}$ and the particles are randomly distributed in pitch, poloidal and toroidal angles. For this case the stochasticity threshold is fairly high since the n=3 eigenmodes peak in a low shear region which increases the field amplitude required for island overlap [11]. Figure 4(b) shows for the $\delta B_r/B=3x10^{-3}$ case the number of particles experiencing a given variation in P_ϕ. The smaller class experiencing a large variation are passing particles while the trapped particles have a small variation in P_ϕ.

ACKNOWLEDGEMENTS

The UKAEA authors were funded by the UK Department of Trade and Industry and by Euratom.

REFERENCES

[1] STRACHAN, J.D., et al., Physical Review Letters **72** (1994) 3526-3529. HAWRYLUK, R.J., et al., ibid. 3530-3533.
[2] FASOLI, A., et al. to be published, also: JET Progress Report 1993, EUR-JET-PR11, p.51.
[3] O'BRIEN, M.R., COX M., WARRICK, C.D., ZAITSEV, F.S., Proceedings of the IAEA Technical Committee Meeting on Advances in Simulation and Modelling of Thermonuclear Plasmas, Montreal 1992, IAEA (1993), p527.
[4] ZAITSEV, F.S., O'BRIEN, M.R., COX, M., Physics of Fluids B **5** (1993) 509-519.
[5] KERNER, W., et al., Plasma Phys. Contr. Fus. **36** (1994), 911.
[6] BETTI, R., FREIDBERG, J.P., Phys. Fluids B **4**, (1992) 1465.
[7] GORELENKOV, N.N., SHARAPOV,S.E. , Phys. Scr. **45**, (1992) 163.
[8] CANDY, J., ROSENBLUTH, M.N. Phys. of Plasmas 1, (1994) 356.
[9] METT, R.R. ,MAHAJAN, S., Phys. Fluids B4 (1992) 2885.
[10] SIGMAR, D.J., HSU, C.T., WHITE, R., CHEING, C.Z., Physics of Fluids B **4** (1992) 1506.
[11] BERK, H.L., BREIZMAN, B.N., Ye, H., Physics of Fluids B **5** (1993) 1506.

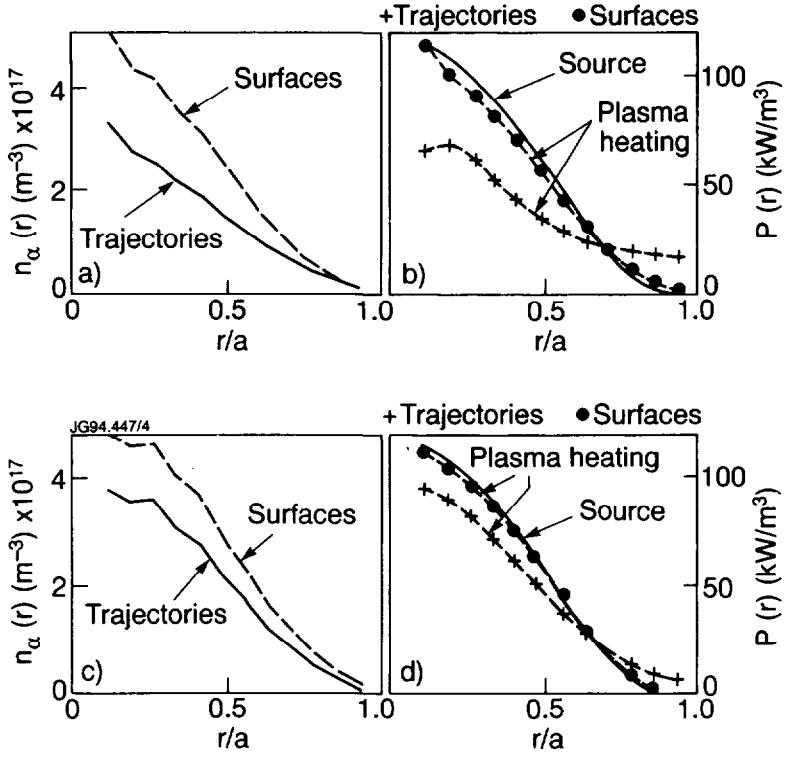

Fig. 1 *Comparison between surface- and trajectory-averaged calculations for I_p=1MA: (a) Alpha-particle density profile and (b) Alpha-particle source and plasma heating profiles, (c) and (d) as (a) and (b) but for I_p=3MA.*

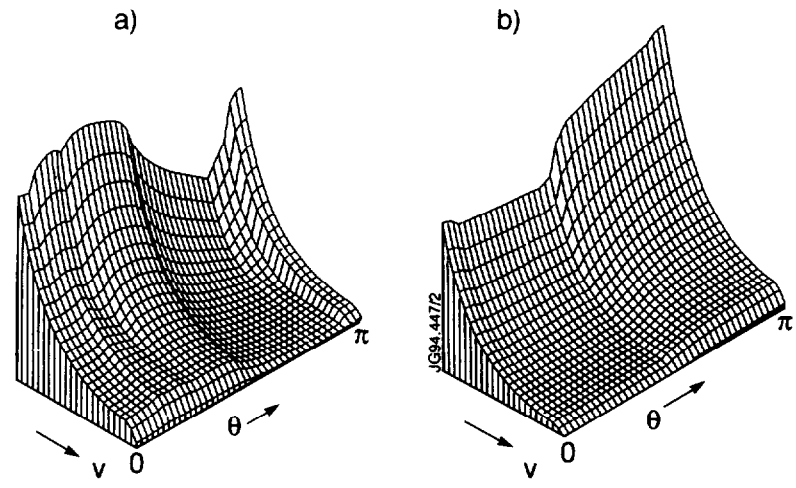

Fig. 2 *Contours of f_α as functions of speed and pitch-angle for I_p=3MA for the (a) outside and (b) inside of the flux surface with r≈a/2. The minimum and maximum energies plotted are 0.6 and 4 MeV.*

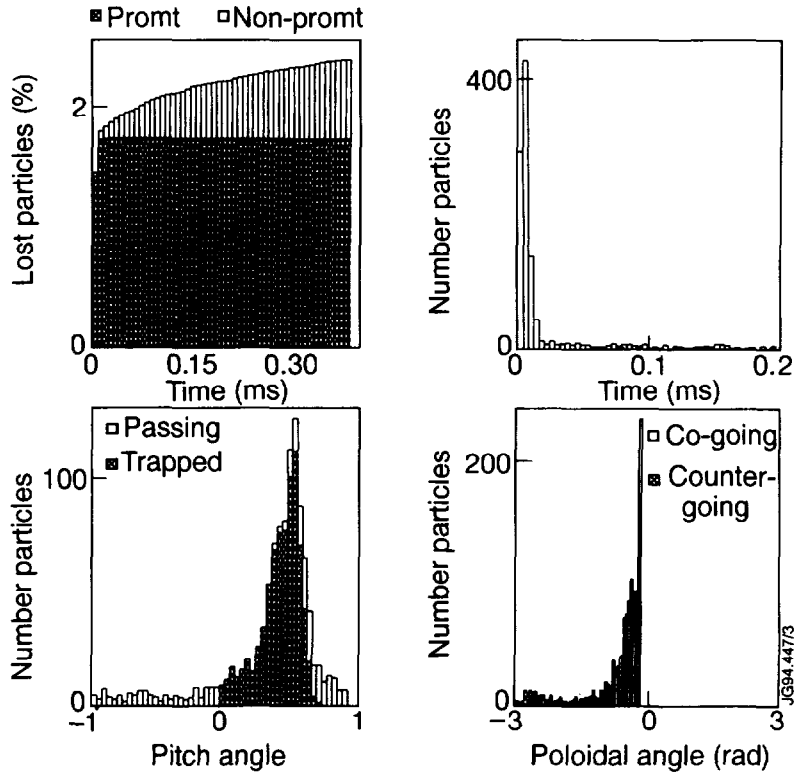

Fig. 3 *(a) Fraction of lost particles as function of time (b) Number of lost particles in 4μs bins with the birth type of the particles distinguished (c) and (d) total number of lost particles versus pitch angle and poloidal angle, respectively.*

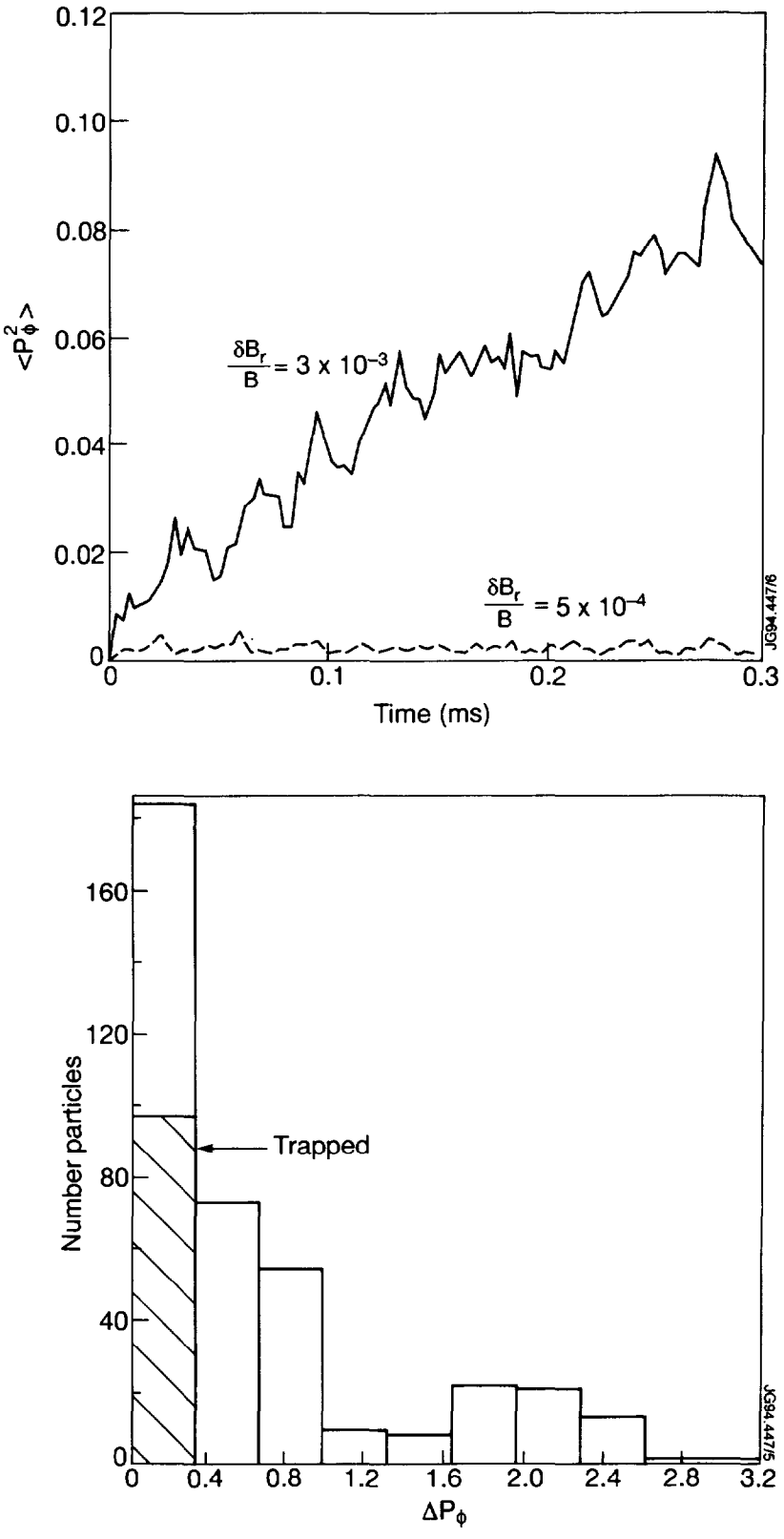

Fig. 4 *(a) Variation of $\langle \Delta P_\phi^2 \rangle x10^{+40}$ with time for $\delta B_r/B=3x10^{-3}$ and $5x10^{-4}$ (b) Number of particles with a given variation ΔP_ϕ for $\delta B_r/B=3x10^{-3}$, the shaded bars are trapped particles.*